Available online at www.sciencedirect.com
ScienceDirect
Trans. Nonferrous Met. Soc. China 23(2013) 3584−3591
Transactions of Nonferrous Metals Society of China
www.tnmsc.cn

Effect of heat treatment on microstructure and thermophysical properties of diamond/2024 Al composites

Zi-yang XIU[1], Xu WANG[2], M. HUSSAIN[3], Chao FENG[1], Long-tao JIANG[1]

1. State Key Laboratory of Advanced Welding and Joining, Harbin Institute of Technology, Harbin 150001, China;
2. School of Mechanical Engineering, Liaoning Shihua University, Fushun 113001, China;
3. Department of Chemical Engineering, COMSATS Institute of Information Technology, Lahore 54000, Pakistan

Received 17 April 2013; accepted 5 July 2013

Abstract: 50% diamond particle (5 μm) reinforced 2024 aluminum matrix (diamond/2024 Al) composites were prepared by pressure infiltration method. Diamond particles were distributed uniformly without any particle clustering, and no apparent porosities or significant casting defects were observed in the composites. The diamond−Al interfaces of as-cast and annealed diamond/2024 Al composites were clean, smooth and free from interfacial reaction product. However, a large number of Al_2Cu precipitates were found at diamond−Al interface after aging treatment. Moreover, needle-shaped Al_2MgCu precipitates in Al matrix were observed after aging treatment. The coefficient of thermal expansion (CTE) of diamond/2024 Al composites was about 8.5×10^{-6} °C^{-1} between 20 and 100 °C, which was compatible with that with chip materials. Annealing treatment showed little effect on thermal expansion behavior, and aging treatment could further decrease the CTE of the composites. The thermal conductivity of obtained diamond/2024 Al composites was about 100 W/(m·K), and it was slightly increased after annealing while decreased after aging treatment.

Key words: Al matrix composites; diamond; interface; annealing; aging; thermal properties

1 Introduction

Ever-growing requirements imposed on thermal management materials in semiconductor applications drive the development of new materials with enhanced thermal conductivity [1,2]. High-performance thermal management materials should have high thermal conductivity (TC) [3,4] to maximize heat dissipation and low coefficient of thermal expansion (CTE) [5,6] to minimize the thermal stress and warping, which are critical issues in packaging of electronic devices [7]. However, the traditional packaging materials such as W/Cu and Mo/Cu could not meet these requirements [8,9]. Therefore, a large effort has been made to develop new materials with improved thermal properties.

Metal-matrix composites (MMCs) with tailored properties have been widely investigated recently. Aluminum matrix composites reinforced with high fraction of SiC [10−12] or Si_3N_4 particles [13,14] demonstrated compatible CTE with chip materials. However, their heat conduction and heat spreading capacity could not meet well with the increasing requirement [15]. Diamond particles have been identified as a promising reinforcement due to their exceptional high TC and low CTE [16], typically 600−2000 W/(m·K) and 0.8×10^{-6} °C^{-1} at 25 °C, respectively.

Pressureless metal infiltration [17,18], spark plasma sintering [7,19,20], powder metallurgy method [21], vacuum hot pressing [22], gas pressure infiltration [23−25] and pressure infiltration method (squeeze casting) [26,27] have been reported to fabricate diamond/Al composites. JOHNSON and SONUPARLAK [17] used pressureless metal infiltration to obtain diamond/Al composites. The diamond particulates were coated with SiC prior to infiltration to prevent the formation of Al_4C_3. Moreover, TC of diamond/Al composites prepared by spark plasma sintering reached 403 W/(m·K) [7,19,20]. HANADA et al [21] reported the processing of diamond/Al with mean particle size of 5 nm by powder metallurgy method. The addition of 1% (volume fraction) cluster diamond improved the friction coefficient of

Foundation item: Project (AWJ-M13-15) supported by the Open Fund of State Key Laboratory of Advanced Welding and Joining, Harbin Institute of Technology, China
Corresponding author: Zi-yang XIU; Tel: +86-451-86402373-5056; E-mail: xiuzy@hit.edu.cn
DOI: 10.1016/S1003-6326(13)62904-0

Al matrix significantly. Furthermore, gas pressure infiltration was also adopted to prepare diamond/Al composites. However, the long exposure time of diamond to molten aluminum led to excessive formation of Al_4C_3, which was observed to be formed with a strong crystallographic preference on the {100} faces of diamond [24]. Therefore, Ti [28] or TiN [29] coatings were used to prevent the formation of Al_4C_3. Pressure infiltration method is believed to be an effective technique because of the advantages of higher production rate, elimination of expensive equipments, feasibility of mass production and near-net products [30,31]. BEFFORT et al [26] investigated the thermal and chemical stability of micron-grade diamond powders as well as the interface microstructure in diamond/Al composites produced by pressure infiltration method. It was found that diamond powders were particularly susceptible to thermal degradation in the presence of oxygen during composite processing, which leads to the formation of an amorphous layer consisting of carbon, aluminum and oxygen.

Our research group has successfully fabricated carbon fibre [32,33] and ceramic particles [13,14] reinforced Al composites by pressure infiltration method under protective atmosphere. Moreover, it is well known that the heat treatment has significant effects on microstructure and properties of metal and metal matrix composites [34,35]. However, the effect of heat treatment on microstructure and properties of diamond/Al composites has rarely been investigated. Therefore, in the present work, 50% (volume fraction) diamond particle (5 μm) reinforced 2024 aluminum matrix composites were prepared by pressure infiltration method. The effect of annealing and aging on microstructure and thermo-physical properties was also discussed.

2 Experimental

The synthetic diamond particles (SF Diamond Co., Ltd., China) with an average particle size of 5 μm were used to reinforce 2024 Al alloy by pressure infiltration method. The basic properties of diamond particles and 2024 Al alloy are shown in Table 1. The chemical composition (mass fraction, %) of the 2024 Al alloy was 4.79% Cu, 1.49% Mg, 0.611% Mn, 0.245% Fe, 0.168% Si, 0.068% Zn, 0.049% Cr, 0.046% Ti, 0.013% Ni and Al balance. A preform comprising diamond particles was prepared firstly. Preheating temperatures for the preform and pressure infiltration dies were 500 and 740−750 °C, respectively. The matrix alloy was melted under protection of argon and melted salts, and poured into dies at 740−750 °C under argon.

Table 1 Properties of diamond particles and 2024 Al alloy

Material	Density/ $(g\cdot cm^{-3})$	Elastic modulus/ GPa	CTE/ $(10^{-6}\ °C^{-1})$	TC/ $(W\cdot m^{-1}\cdot K^{-1})$
Diamond particles	3.52	435	1.7	900−1100
2024 Al alloy	2.82	68	21.1−24.7	134−192

The schematic diagrams of annealing and aging treatment are shown in Fig. 1. The annealing samples were held at 360 °C for 1 h and then cooled in the furnace to room temperature. The aging samples were solution treated at 495 °C in KNO_3 salt-bath furnace for 1 h and water quenched at room temperature. After solution treatment, specimens were aged at 190 °C for 8 h and cooled in the air. The as-cast samples were used for comparison.

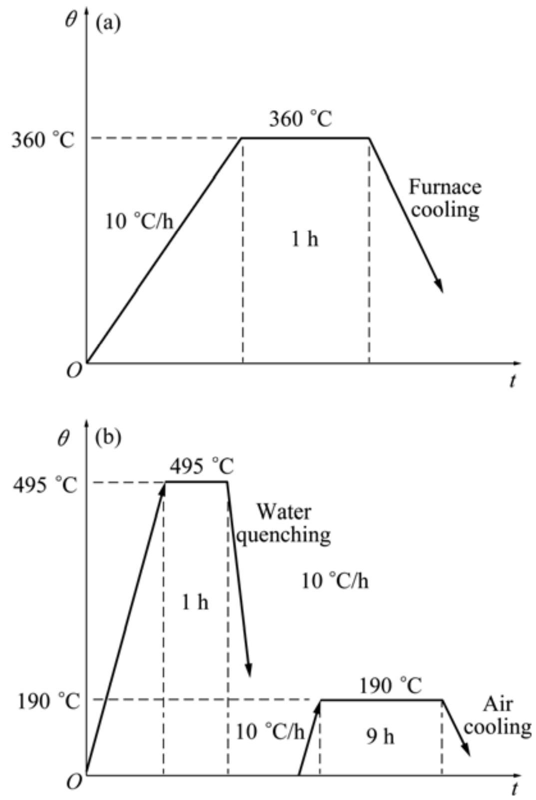

Fig. 1 Schematic diagrams of annealing (a) and aging (b) treatment

The density of diamond/2024 Al composites was measured by Archimedes' method. The morphology of diamond/2024 Al composites was observed by ZEISS 40MAT optical microscope (OM) and FEI Sirion Quanta 200 scanning electron microscope (SEM). Further microstructure observation was conducted by a Philips CM−12 transmission electron microscope (TEM) with an accelerated voltage of 100−120 kV. Thermal conductivity (TC) and specific heat capacity of the composite and matrix, with a diameter of 12.7 mm and a thickness of 2 mm, were examined on LFA 427 laser flash apparatus (Netzsch, Germany) from 20 to 50 °C with a heating rate of 5 °C/min. CTE tests were carried out on Dilatometer 402C (Netzsch, Germany). The samples were the cylinders with a diameter of 4 mm and a length of 25 mm. During the CTE measurement, the temperature was increased from 20 to 495 °C at a heating rate of 5 °C/min. The helium atmosphere was maintained at a flow rate of 50 mL/min to ensure the equilibrium of temperature and prevent oxidation of samples.

3 Results and discussion

3.1 Microstructure

The irregular shape diamond particles were used in the present work, as shown in Fig. 2. The representative optical morphologies of the diamond/2024 Al composites in as-cast, annealed and aged condition are shown in Fig. 3. Diamond particles were distributed uniformly without any particle clustering, and no apparent porosities or significant casting defects were observed in the composites. The dense microstructure is favorable for the mechanical and thermal conductivity properties. Moreover, the dense microstructure is also beneficial to improving the dimensional stability of composite, which would prolong the service life of devise.

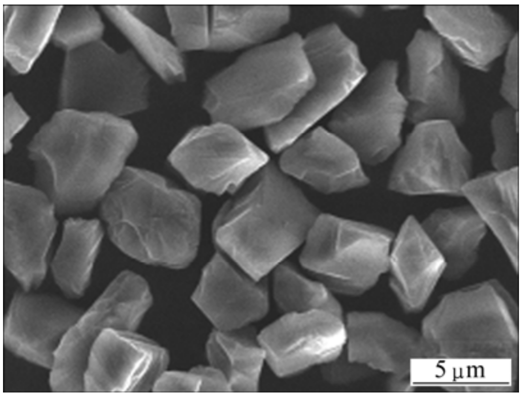

Fig. 2 SEM image of diamond particles used in the present work

Representative SEM images of diamond/2024 Al composites in as-cast, annealed and aged condition are shown in Fig. 4. It is obvious that some diamond particles were polished away due to the large hardness difference between reinforcement and matrix.

TEM images of diamond−Al interface of as-cast, annealed and aged diamond/2024 Al composites are shown in Fig. 5. As reported by BEFFORT et al [24], amorphous interfacial C-layer and excessive Al_4C_3 phases were observed in as-cast diamond/Al composites fabricated by pressure infiltration method. However, in the present work, the diamond−Al interface of as-cast

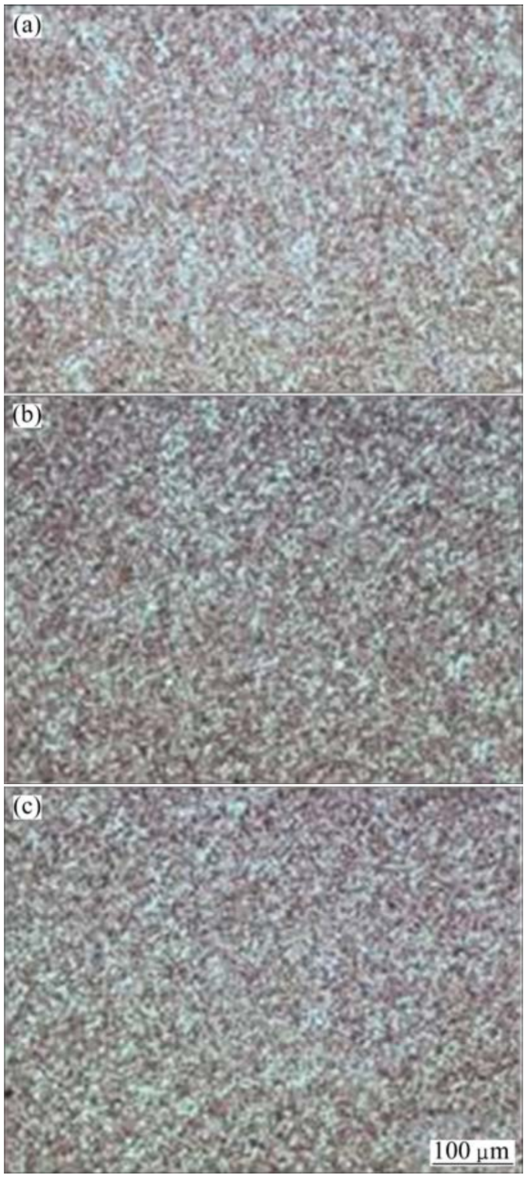

Fig. 3 Optical morphologies of diamond/2024 Al composites in as-cast (a), annealed (b) and aged (c) condition

diamond/2024 Al composites was clean, smooth and free from interfacial reaction product (Fig. 5(a)). Diamond particles would undergo thermal degradation [24]. This effect is more obvious in air atmosphere [27]. Therefore, amorphous carbon and isolated Al carbides were observed in the obtained composites. However, in the present work, the diamond preform was protected by CO_2, which would inhabit its degradation. Therefore, the diamond−Al interface is clean and without amorphous layer and Al_4C_3 phases in as-cast composite. No significant change was observed at diamond−Al interface in annealed composite (Fig. 5(b)). However, a large number of Al_2Cu precipitates were found at diamond−Al interface after aging treatment (Fig. 5(c)). Moreover, it was hard to observe Al_2Cu phase in Al matrix.

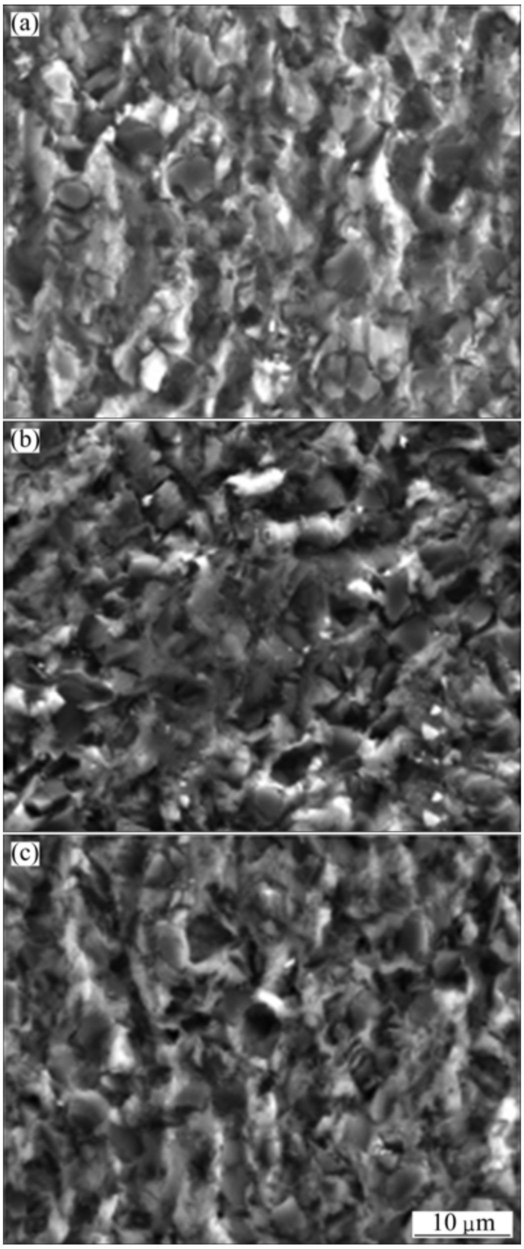

Fig. 4 SEM images of diamond/2024 Al composites in as-cast (a), annealed (b) and aged (c) conditions

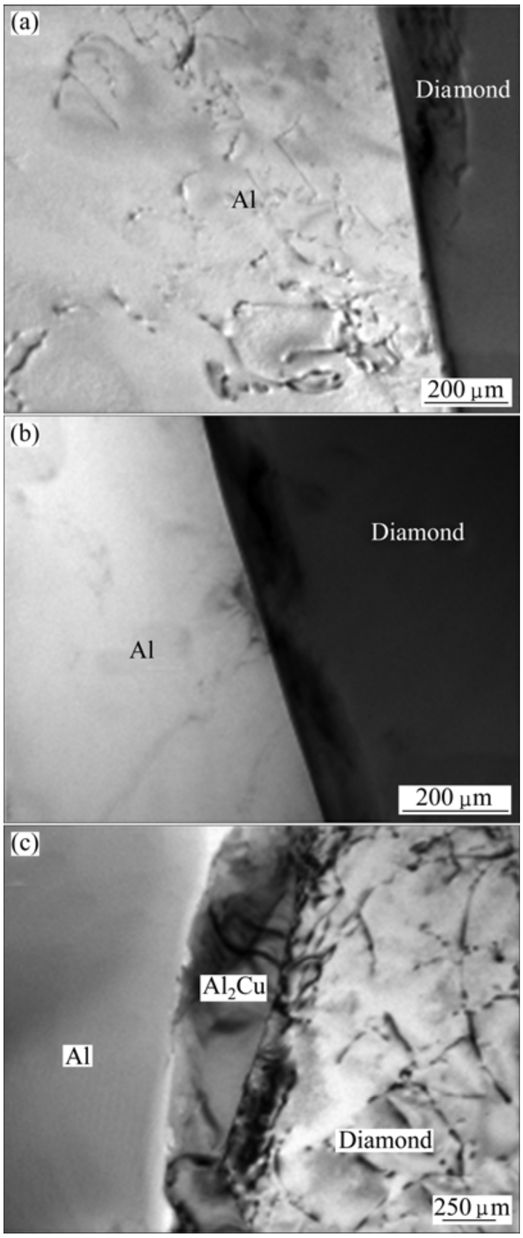

Fig. 5 TEM images of diamond−Al interface of as-cast (a), annealed (b) and aged (c) diamond/2024 Al composites

The diamond−Al interface provides extra energy for heterogeneous nucleation of Al_2Cu, leading to the low nucleation energy and a relatively high nucleation rate at the interface compared with that in Al matrix. Therefore, Al_2Cu phase would grow predominantly at the interface instead of in Al matrix during aging treatment.

The dislocations in Al matrix of as-cast, annealed and aged diamond/2024 Al composites are shown in Fig. 6. Large CTE difference between diamond particles and Al matrix would generate enormous thermal tensile stresses on Al matrix during rapid cooling after Al infiltration, which leads to the formation of high density dislocations near the diamond−Al interface (Fig. 6(a)). The annealing treatment decreased the density of the dislocations significantly due to release of residual thermal stress (Fig. 6(b)). However, more dislocations were found after aging treatment. Water quenching process in aging treatment generates larger thermal stress at diamond−Al interface, which leads to the reformation of dislocations. Moreover, apparent needle-shaped precipitates were found in Al matrix after aging treatment (Fig. 7(a)), and the weak diffraction spots in electron diffraction pattern (Fig. 7(b)) were elongated lines, which corresponds to Al_2MgCu.

Crystal defects in particle reinforcements, which have important influence on interface and properties, are significant characteristics of particle reinforced metal matrix composite. Stacking faults and dislocations have

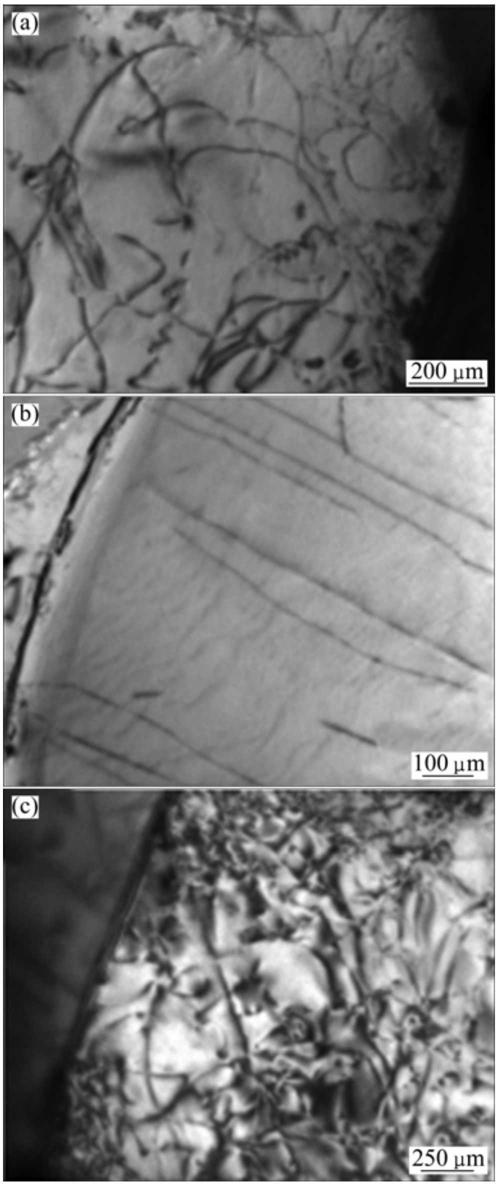

Fig. 6 TEM images of dislocations in Al matrix of as-cast (a), annealed (b) and aged diamond/2024 Al composites (c)

been observed in ceramic particles reinforced Al matrix composites [36,37], the high density dislocations in AlN particles even tangle with each other [38]. In the present work, few aligned linear dislocations (Fig. 8) were found in diamond particles. Generally, the crystal defects in reinforcements are generated in preparation process of particles as well as composites. The diamond particles were fabricated under high temperature and pressure, which may produce some crystal defects. Moreover, the volume fraction of particles was very high (50%), parts of particles contacted with each other during perform densification or Al infiltration under pressure. Since the morphology of the diamond particles was irregular with sharp edges (Fig. 2), some sharp edges would exert pressure to the contacted surface of other particles

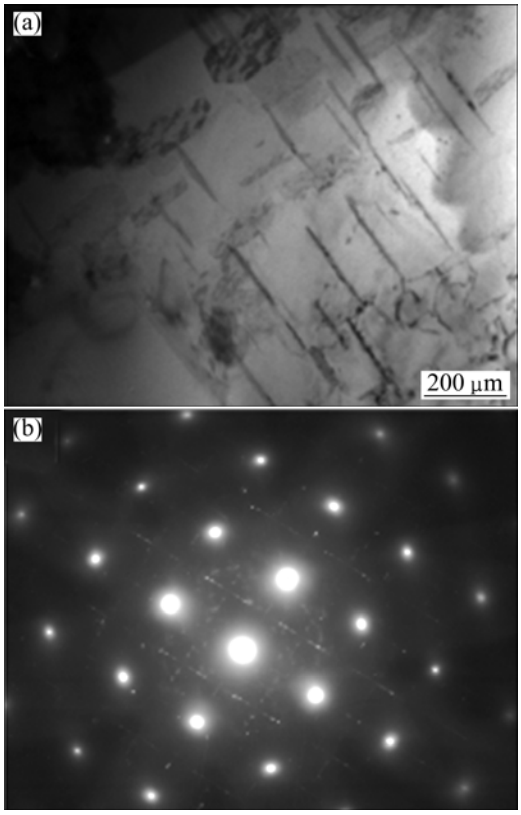

Fig. 7 Al_2MgCu precipitates in Al matrix of diamond/2024 Al composites after aging treatment: (a) TEM image; (b) Electron diffraction pattern

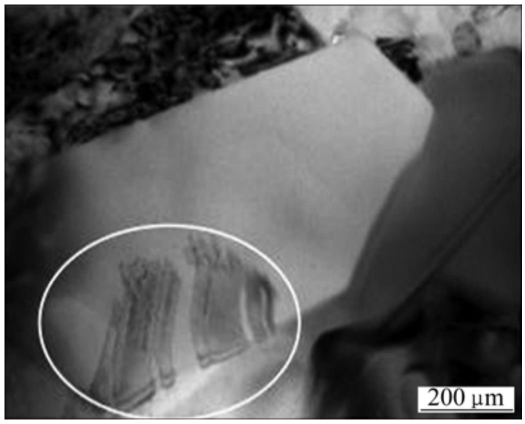

Fig. 8 TEM image of few linear dislocations in diamond particles

inevitably, which would generate dislocations. Furthermore, a large CTE difference between diamond particles and Al matrix would generate enormous thermal compressive stresses on diamond particles, which would also contribute to the formation of dislocations in the diamond particles.

3.2 Thermophysical properties

The CTE comparison of diamond/2024 Al in as-cast, annealed and aged condition is shown in Fig. 9. Regardless of heat treatment, the CTEs of diamond/

2024 Al composite were reduced greatly to nearly half that of the 2024 Al matrix [13] with high addition of diamond particles. It is well known that the thermal expansion of metal matrix composite is determined by the thermal expansion of metal matrix and the restriction of reinforcement through interfaces. High content of diamond particles imposes large restriction on surrounding aluminum matrix, which leads to the low CTE of the diamond/2024 Al composite. Moreover, annealing treatment has little effect on thermal expansion behavior. Aging treatment could further decrease the CTE of the composite. The formation of Al_2Cu phases at diamond−Al interface could improve the interfacial bonding and restriction of diamond particles on the surrounding Al matrix, which leads to the decrease of CTE. Furthermore, formation of Al_2MgCu precipitates in Al matrix could also contribute to the decrease of CTE. The CTE of diamond/2024 Al composite was about 8.5×10^{-6} °C^{-1} between 20 and 100 °C, which is compatible with that of chip materials.

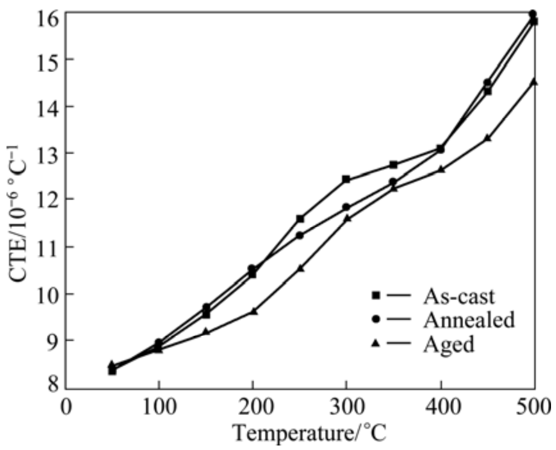

Fig. 9 CTE comparison of as-cast, annealed and aged diamond/2024 Al composites

The thermal diffusivity (α) and conductivity (λ) of diamond/2024 Al composites in as-cast, annealed and aged condition are shown in Table 2. The thermal conductivity of diamond/Al composite is expected to exceed 600 W/(m·K). However, the measured thermal conductivity of the present composite was about 100 W/(m·K), which was far lower than the theoretical value. Although lager particles were adopted (average particle size of 100 μm), thermal conductivity of diamond/Al, which was also fabricated by pressure infiltration method, was about 130 W/(m·K) [14]. The annealing treatment improved the thermal diffusivity and conductivity while aging treatment showed an opposite effect. There are two ways for heat transfer in diamond/2024 Al composite: free electron in Al matrix and phonon in diamond particles. Both of their movements would be scattered by interface. Therefore, heat conduction in diamond/2024 Al composite is depended on Al matrix, diamond particles and their interface. The annealing treatment would release the residual thermal stress in Al matrix generated in fabrication, which is beneficial to heat conduction, and lead to improvement of the thermal conductivity. Moreover, the density of the dislocations decreased after annealing treatment, which also contributed to the increase of TC. However, after aging treatment, more scattering interfaces for electron and phonon were introduced into the composite, such as Al_2Cu phase at diamond−Al interface (Fig. 5(c)), Al_2MgCu precipitates in Al matrix (Fig. 7(a)) and higher density dislocations introduced more interfaces into the composite, which would scatter the movement of electron and phonon, and decrease the thermal conductivity. Therefore, thermal conductivity is slightly decreased after aging treatment.

Table 2 Thermal diffusivity and conductivity of diamond/2024 Al composites after different treatments

Condition	Thermal diffusivity/ ($m^2 \cdot s^{-1}$)	Thermal conductivity/ ($W \cdot m^{-1} \cdot K^{-1}$)
As-cast	42.6	106.7
Annealed	43.7	109.3
Aged	41.0	102.3

4 Conclusions

1) 50% (volume fraction) diamond particle (5 μm) reinforced 2024 aluminum matrix (diamond/2024 Al) composites were prepared by pressure infiltration method. Diamond particles are distributed uniformly without any particle clustering, and no apparent porosities or significant casting defects are observed in the composites.

2) The diamond−Al interfaces of as-cast and annealed diamond/2024 Al composites are clean, smooth and free from interfacial reaction product. However, a large number of Al_2Cu precipitates are found at diamond−Al interface after aging treatment. High density dislocations are observed in the as-cast composite. The density of dislocations is decreased and increased after annealing and aging treatment, respectively.

3) The CTE of diamond/2024 Al composites is about 8.5×10^{-6} °C^{-1} between 20 and 100 °C, which is compatible with that of chip materials. Annealing treatment has little effect on thermal expansion behavior, and aging treatment can further decrease the CTE of the composite.

4) The thermal conductivity of obtained diamond/2024 Al composites is about 100 W/(m·K). Due to the release of residual stress and decrease of dislocations, thermal conductivity of diamond/2024 Al composites slightly increases after annealing treatment. However,

thermal conductivity of diamond/2024 Al composites slightly decreases the formation of Al_2Cu at diamond−Al interface and Al_2MgCu precipitates in Al matrix.

References

[1] RAPE A, LIU X, KULKARNI A, SINGH J. Alloy development for highly conductive thermal management materials using copper-diamond composites fabricated by field assisted sintering technology [J]. Journal of Materials Science, 2013, 48(3): 1262−1267.

[2] SINHA V, SPOWART J E. Influence of interfacial carbide layer characteristics on thermal properties of copper–diamond composites [J]. Journal of Materials Science, 2013, 48(3): 1330−1341.

[3] RAPE A, CHANTHAPAN S, SINGH J, KULKAMI A. Engineered chemistry of Cu−W composites sintered by field-assisted sintering technology for heat sink applications [J]. Journal of Materials Science, 2011, 46(1): 94−100.

[4] WEI Xing-hai, LIU Lang, ZHANG Jin-xi, SHI Jing-li, GUO Quan-gui. Mechanical, electrical, thermal performances and structure characteristics of flexible graphite sheet [J]. Journal of Materials Science, 2010, 45(9): 2449−2455.

[5] JIANG Lan, JIANG Yan-li, YU Liang, SU Nan, DING You-dong. Thermal analysis for brake disks of SiC/6061 Al alloy co-continuous composite for CRH3 during emergency braking considering airflow cooling [J]. Transactions of Nonferrous Metals Society of China, 2012, 22(11): 2783−2791.

[6] ZHANG Qiang, WU Gao-hui, JIANG Long-tao, CHEN Guo-qing. Thermal expansion and dimensional stability of Al−Si matrix composite reinforced with high content SiC [J]. Materials Chemistry and Physics, 2003, 82(3): 780−785.

[7] MIZUUCHI K, INOUE K, AGARI Y, MORISADA Y, SUGIOKA M, TANAKA M, TAKEUCHI T, KAWAHARA M, MAKINO Y. Thermal conductivity of diamond particle dispersed aluminum matrix composites fabricated in solid–liquid co-existent state by SPS [J]. Composites Part B: Engineering, 2011, 42(5): 1029−1034.

[8] CHEN Hui, JIA Cheng-chang, LI Shang-jie. Interfacial characterization and thermal conductivity of diamond/Cu composites prepared by two HPHT techniques [J]. Journal of Materials Science, 2012, 47(7): 3367−3375.

[9] ABYZOV A M, KIDALOV S V, SHAKHOV F M. High thermal conductivity composites consisting of diamond filler with tungsten coating and copper (silver) matrix [J]. Journal of Materials Science, 2011, 46(5): 1424−1438.

[10] ZHANG Gui-feng, SU Wei, ZHANG Jian-xun, SUZUMURA A. Development of Al−12Si−*x*Ti system active ternary filler metals for Al metal matrix composites [J]. Transactions of Nonferrous Metals Society of China, 2012, 22(3): 596−603.

[11] CHEN Guo-xin, XIU Zi-yang, YANG Wen-shu, JIANG Long-tao, WU Gao-hui. Effect of thermal-cooling cycle treatment on thermal expansion behavior of particulate reinforced aluminum matrix composites [J]. Transactions of Nonferrous Metals Society of China, 2010, 20(11): 2143−2147.

[12] WEBER L, SINICCO G, MOLINA J M. Influence of processing route on electrical and thermal conductivity of Al/SiC composites with bimodal particle distribution [J]. Journal of Materials Science, 2010, 45(8): 2203−2209.

[13] CHEN Guo-qing, YANG Wen-shu, MA Kang, HUSSAIN M, JIANG Long-tao, WU Gao-hui. Aging and thermal expansion behavior of Si_3N_{4p}/2024Al composite fabricated by pressure infiltration method [J]. Transactions of Nonferrous Metals Society of China, 2011, 21(S2): s262−s273.

[14] XIU Zi-yang, YANG Wen-shu, CHEN Guo-qing, JIANG Long-tao, MA Kang, WU Gao-hui. Microstructure and tensile properties of Si3N4p/2024Al composite fabricated by pressure infiltration method [J]. Materials & Design, 2012, 33: 350−355.

[15] DONG Ying-hu, HE Xin-bo, RAFI-UD-DIN, XU Liang, QU Xuan-hui. Fabrication and thermal conductivity of near-net-shaped diamond/copper composites by pressureless infiltration [J]. Journal of Materials Science, 2011, 46(11): 3862−3867.

[16] KHALID F A, BEFFORT O, KLOTZ U E, KELLER B A, GASSER P. Microstructure and interfacial characteristics of aluminium–diamond composite materials [J]. Diamond and Related Materials, 2004, 13(3): 393−400.

[17] JOHNSON W B, SONUPARLAK B. Diamond/Al metal matrix composites formed by the pressureless metal infiltration process [J]. Journal of Materials Research, 1993, 8(5): 1169−1173.

[18] SHI J, CHE R C, LIANG C Y, CUI Y, XU S B, ZHANG L. Microstructure of diamond/aluminum composites fabricated by pressureless metal infiltration [J]. Composites Part B: Engineering, 2011, 42(6): 1346−1349.

[19] MIZUUCHI K, INOUE K, AGARI Y, MORISADA Y, SUGIOKA M, TANAKA M, TAKEUCHI T, TANI J I, KAWAHARA M, MAKINO Y. Processing of diamond particle dispersed aluminum matrix composites in continuous solid–liquid co-existent state by SPS and their thermal properties [J]. Composites Part B: Engineering, 2011, 42(4): 825−831.

[20] MIZUUCHI K, INOUE K, AGARI Y, SUGIOKA M, TANAKA M, TAKEUCHI T, KAWAHARA M, MAKINO Y, ITO M. Processing of diamond-particle-dispersed silver-matrix composites in solid–liquid co-existent state by SPS and their thermal conductivity [J]. Composites Part B: Engineering, 2012, 43(3): 1445−1452.

[21] HANADA K, MAYUZUMI M, NAKAYAMA N, SANO T. Processing and characterization of cluster diamond dispersed Al−Si−Cu−Mg composite [J]. Journal of Materials Processing Technology, 2001, 119(1−3): 216−221.

[22] TAN Zhan-qiu, LI Zhi-qiang, FAN Gen-lian, KAI Xi-zhou, JI Gang, ZHANG Lan-ting, ZHANG Di. Fabrication of diamond/aluminum composites by vacuum hot pressing: Process optimization and thermal properties [J]. Composites Part B: Engineering, 2013, 47: 173−180.

[23] BATTABYAL M, BEFFORT O, KLEINER S, VAUCHER S, ROHR L. Heat transport across the metal–diamond interface [J]. Diamond and Related Materials, 2008, 17(7−10): 1438−1442.

[24] BEFFORT O, KHALID F A, WEBER L, RUCH P, KLOTZ U E, MEIERD S, KLEINER S. Interface formation in infiltrated Al(Si)/diamond composites [J]. Diamond and Related Materials, 2005, 9(36): 1250−1260.

[25] XUE C, YU J K, ZHU X M. Thermal properties of diamond/SiC/Al composites with high volume fractions [J]. Materials & Design, 2011, 32(8−9): 4225−4229.

[26] BEFFORT O, LONG S, CAYRON C, KUEBLER J, BUFFAT P A. Alloying effects on microstructure and mechanical properties of high volume fraction SiC-particle reinforced Al-MMCs made by squeeze casting infiltration [J]. Composites Science and Technology, 2007, 67(3−4): 737−745.

[27] RUCH P W, BEFFORT O, KLEINER S, WEBER L, UGGOWITZER P J. Selective interfacial bonding in Al(Si)–diamond composites and its effect on thermal conductivity. [J]. Composites Science and Technology, 2006, 66(15): 2677−2685.

[28] YANG Bo, YU Jia-kang, CHEN Chuang. Microstructure and thermal expansion of Ti coated diamond/Al composites [J]. Transactions of Nonferrous Metals Society of China, 2009, 19(5): 1167−1173.

[29] FENG H, YU J K, TAN W. Microstructure and thermal properties of diamond/aluminum composites with TiC coating on diamond particles [J]. Materials Chemistry and Physics, 2010, 124(1): 851−855.

[30] WU G H, SU J, GOU H S, XIU Z Y, JIANG L T. Study on graphite fiber and Ti particle reinforced Al composite [J]. Journal of Materials Science, 2009, 44(18): 4776−4780.
[31] LIU Y M, XIU Z Y, WU G H, YANG W S, CHEN G Q, GOU H S. Study on Ti fiber reinforced TiAl3 composite by infiltration-in situ reaction [J]. Journal of Materials Science, 2009, 44(16): 4258−4263.
[32] WANG Xu, CHEN Guo-qin, YANG Wen-shu, HUSSAIN M, WANG Chen-chong, WU Gao-hui, JIANG Da-ming. Effect of Nd content on microstructure and mechanical properties of Grf/Al composite [J]. Materials Science and Engineering A, 2011, 528(28): 8212−8217.
[33] XIU Z Y, CHEN G Q, WANG M, HUSSAIN M. Effect of TiN coating on microstructure of Tif/Al composite [J]. Micron, 2013, 45: 92−96.
[34] YANG Xin, SU Zhe-an, HUANG Qi-zhong, CHAI Li-yuan. Preparation and oxidation resistance of mullite/SiC coating for carbon materials at 1150 °C [J]. Transactions of Nonferrous Metals Society of China, 2012, 22(12): 2997−3002.
[35] YANG Li-jing, WEI Ying-hui, HOU Li-feng. Microstructure evolution of thixomolding AZ91D magnesium alloy during heat treatment [J]. Journal of Materials Science, 2010, 45(13): 3626−3634.
[36] EL-DALY A A, ABDELHAMEED M, HASHISH M, DAOUSH W M. Fabrication of silicon carbide reinforced aluminum matrix nanocomposites and characterization of its mechanical properties using non-destructive technique [J]. Materials Science and Engineering A, 2013, 559: 384−393.
[37] BATHULA S, ANANDANI R C, DHAR A, SRIVASTAVA A K. Microstructural features and mechanical properties of Al 5083/SiCp metal matrix nanocomposites produced by high energy ball milling and spark plasma sintering. [J]. Materials Science and Engineering A, 2012, 545: 97−102.
[38] ZHAO Min, WU Gao-hui, ZHU De-zhi, JIANG Long-tao, DOU Zuo-yong. Effects of thermal cycling on mechanical properties of AlN_p/Al composite [J]. Materials Letters, 2004, 58(12−13): 1899−1902.

热处理对金刚石/2024Al 复合材料微观组织和热物理性能的影响

修子扬[1]，王 旭[2]，M. HUSSAIN[3]，冯 超[1]，姜龙涛[1]

1. 哈尔滨工业大学 先进焊接与连接国家重点实验室，哈尔滨 150001；
2. 辽宁石油化工大学 机电学院，抚顺 113001；
3. Department of Chemical Engineering, COMSATS Institute of Information Technology, Lahore 54000, Pakistan

摘 要：采用挤压铸造法制备粒径为 5 μm、体积分数为 50%的金刚石/2024Al 复合材料。退火处理后对其金相组织界面反应、界面结合情况以及金刚石颗粒的内部缺陷进行观察与分析，并对其热物理性能进行测试与研究。结果表明，金刚石/2024Al 复合材料的组织致密，无明显的气孔、夹杂等缺陷；颗粒为不规则多边形，有棱角，分布比较均匀。透射电镜观察表明，部分金刚石颗粒内部有位错和层错存在，而 2024Al 基体中的位错密度较大，金刚石/2024Al 界面处有较多的界面反应物生成，可能为 Al_2Cu。复合材料在 20~100 °C 温度区间内的平均热膨胀系数为 8.5×10^{-6} °C^{-1}，退火处理的复合材料其热膨胀系数有一定程度的降低；随着温度的升高，复合材料的平均热膨胀系数也呈现增加的趋势。复合材料的热导率约为 100 W/(m·K)，退火处理能够提高复合材料的热导率。
关键词：铝基复合材料；金刚石；界面；退火；时效；热物理性能

(Edited by Xiang-qun LI)